

Bioactive *ent*-kaurane diterpenoids from *Isodon serra*



Jun Wan^{a, b}, Miao Liu^{a, b}, Hua-Yi Jiang^{a, b}, Jin Yang^{a, b}, Xue Du^a, Xiao-Nian Li^a, Wei-Guang Wang^a, Yan Li^a, Jian-Xin Pu^{a, *}, Han-Dong Sun^a

^a State Key Laboratory of Phytochemistry and Plant Resources in West China, Kunming Institute of Botany, Chinese Academy of Sciences, Kunming 650201, PR China

^b University of Chinese Academy of Sciences, Beijing 10039, PR China

ARTICLE INFO

Article history:

Received 24 December 2015

Received in revised form

25 May 2016

Accepted 31 May 2016

Available online 10 June 2016

Keywords:

Isodon serra

Lamiaceae

7,20-Epoxy-*ent*-kaurane diterpenoids

Cytotoxic activity

Anti-inflammatory

ABSTRACT

Nine 7,20-epoxy-*ent*-kaurane diterpenoids (15-acetylmegathyrin B, serrin E, 14 β -hydroxyrabdocoestin A, serrin F, serrin G, 11-*epi*-rabdocoestin A, serrin H, serrin I, and 15-acetylenanderianin N), along with seven known ones, were isolated from the aerial parts of *Isodon serra*. Their structures were elucidated by extensive spectroscopic analysis, and the absolute configuration of 15-acetylmegathyrin B was determined by signal-crystal X-ray diffraction. All of these compounds were evaluated for their cytotoxic activities against five human tumor cell lines (HL-60, SMMC-7721, A-549, MCF-7, SW480). Serrin F, rabdocoestin B and 1 α ,11 β -dihydroxy-1 α ,11 β -acetone-7 α ,20-epoxy-*ent*-kaur-16-en-15-one showed cytotoxic activities against all cell lines, with IC₅₀ values ranging from 0.7 to 4.6 μ M; serrin F also strongly inhibited NO production in LPS-stimulated RAW264.7 cells. Otherwise, 14 β -hydroxyrabdocoestin A, serrins H and I, as well as enanderianin N and megathyrin B, also exhibited inhibitory effects towards NO production, while no cytotoxicity against five cell lines was detected.

© 2016 Elsevier Ltd. All rights reserved.

1. Introduction

The genus *Isodon*, including about 150 species, has been investigated for its abundant diterpenoid constituents and their biological activities for over half a century since the determination of its enmein structure (Sun et al., 2001, 2006; Ikeda and Kanatomo, 1958; Iitaka and Natsume, 1964; Fukita et al., 1965). *Isodon serra* (Maxim.) Hara, also called 'Xihuangcao' in Chinese folk medicine, is mainly distributed in Guangdong, Fujian and Jiangxi Provinces of China, and has long been used to treat jaundice hepatitis, acute cholecystitis, and enteritis (Zhong Yao Da Ci Dian, 1997; Flora of China, 1977; Wong et al., 2015). Previous phytochemical investigations of *I. serra* from different regions of China led to the isolation of a variety of *ent*-kaurane types, including enmein, spiro-lactone, C-20-non-oxygenated, and C-20-oxygenated-kauranoids types (Jin et al., 1985; Zhao et al., 2004; Yan et al., 2007; Du et al., 2011; Zheng et al., 2011; Yan et al., 2012). Among them, serrins A–C showed immunosuppressive effects towards T-lymphocytes (Zhao et al., 2004), and rabdoserin B exhibited inhibitory activity to human retinoblastoma cells (Jin et al., 1987; Hai et al., 2010).

In an ongoing search for bio-active diterpenoids from the genus *Isodon*, the chemical constituents of *I. serra*, collected from the E'mei mountain, Sichuan Province, were investigated. This study led to isolation of nine new *ent*-kauranoids, 15-acetylmegathyrin B (**1**), serrin E (**2**), 14 β -hydroxyrabdocoestin A (**3**), serrin F (**4**), serrin G (**5**), 11-*epi*-rabdocoestin A (**6**), serrin H (**7**), serrin I (**8**), and 15-acetylenanderianin N (**9**), as well as seven known ones (**10**–**16**), rabdocoestin A (**10**) (Xu et al., 1993), rabdocoestin B (**11**) (Chen et al., 1990), enanderianin N (**12**) (Xiang et al., 2003), 1 α ,11 β -dihydroxy-1 α ,11 β -acetone-7 α ,20-epoxy-*ent*-kaur-16-en-15-one (**13**) (Chen et al., 1990), megathyrin A (**14**) (Sun et al., 1994), enanderianin L (**15**) (Xiang et al., 2003) and megathyrin B (**16**) (Qiu et al., 1998) (Fig. 1). Due to the potent antitumor activities of the *ent*-kauranoids isolated from this genus (Sun et al., 2006), all of these compounds were evaluated for both their cytotoxic activities against five human tumor cell lines (HL-60, SMMC-7721, A-549, MCF-7, SW480) (Table 3) and their NO production inhibitory activities in LPS-stimulated RAW264.7 cells (Table 4). In this paper, the isolation, structure elucidation, cytotoxic activities and NO production inhibitory activities of these diterpenoids are reported.

2. Results and discussion

A 70% aqueous acetone extract of the air-dried and powdered

* Corresponding author.

E-mail address: pujianxin@mail.kib.ac.cn (J.-X. Pu).

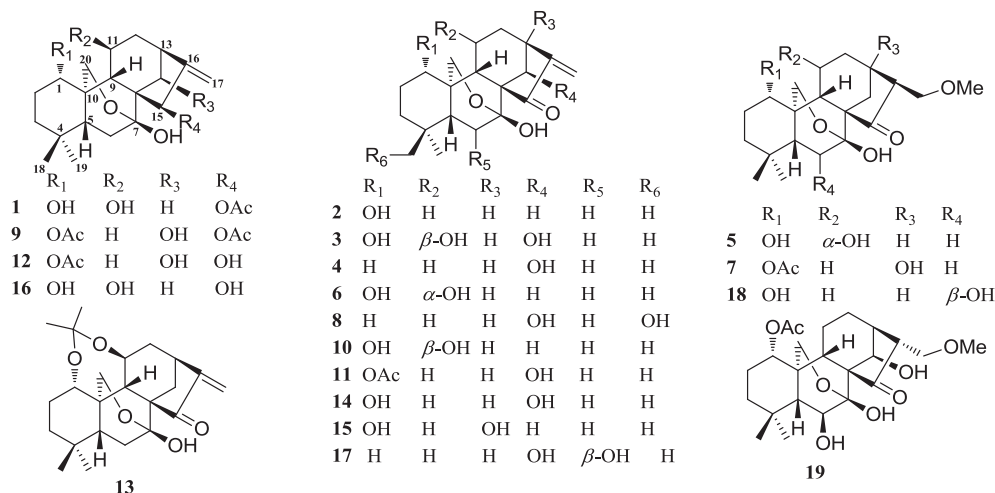


Fig. 1. Structures of compounds 1–19.

aerial parts of *I. serra* was partitioned between EtOAc and H₂O. The EtOAc layer was subjected to repeated column chromatography and then HPLC to afford 9 new 7,20-epoxy-*ent*-kauranoids, named 15-acetylmegathyrin B (**1**), serrin E (**2**), 14 β -hydroxyrabdocoestin A (**3**), serrin F (**4**), serrin G (**5**), 11-*epi*-rabdocoestin A (**6**), serrin H (**7**), serrin I (**8**), and 15-acetylenanderianin N (**9**), respectively.

Compound **1** was obtained as colorless crystals (MeOH). Its molecular formula was deduced to be C₂₂H₃₂O₆ by its HRESIMS ([M+Na]⁺ *m/z* 415.2093, calcd 415.2091), corresponding to seven degrees of unsaturation. Its IR spectrum disclosed the existence of hydroxy (3355 cm⁻¹), acetoxy carbonyl (1744 cm⁻¹), and olefinic groups (1632 cm⁻¹). The ¹H NMR (Table 1) spectrum showed resonances attributed to the characteristic AB methylene group at δ_{H} 4.57 and δ_{H} 4.81 (each 1H, d, *J* = 10.0 Hz), and three quaternary methyls at δ_{H} 0.77 (3H, s), δ_{H} 1.08 (3H, s), and δ_{H} 2.16 (3H, s). The ¹³C NMR and DEPT (Table 2) spectra of **1** exhibited 22 carbon signals, including three methyls, seven methylenes (one oxygenated), six methines (three oxygenated) and six quaternary carbons (one oxygenated, one lactonic carbonyl carbon). These resonances suggested that **1** possessed a 7,20-epoxy-*ent*-kauranoid skeleton similar to that of megathyrin B (**16**), except that C-15 was substituted by an acetoxy group in **1**. Comparisons of the NMR spectroscopic data of **1** and **16** indicated that **1** differed from **16** by possessing one more methyl (δ_{H} 2.16, 3H, s) and acetyl carbon signals (δ_{C} 170.7, s), which was supported by the following 2D NMR correlations and its unsaturation degrees: (i) the ¹H–¹H COSY spectrum showed correlations of H-1/H₂-2/H₂-3 and H-11/H₂-12/H-13/H₂-14 (Fig. 2); (ii) HMBC correlations from H₂-2 (δ_{H} 1.90, 2H, m), H₂-3 (δ_{H} 1.44 and 1.25), H-5 (δ_{H} 1.69), H-9 (δ_{H} 2.47), and H₂-20 (δ_{H} 4.57, 4.81) to C-1 (δ_{C} 73.8, d), and from H-9 (δ_{H} 2.47), H₂-12 (δ_{H} 2.85 and 1.83), and H-13 (δ_{H} 2.68) to C-11 (δ_{C} 63.0, d) implied the positions of OH-1 and OH-11; (iii) HMBC correlations from H₂-14 (δ_{H} 2.09, 2H), H₂-17 (δ_{H} 5.12, 2H, br s), and CH₃-OAc (δ_{H} 2.16, 3H, s) to C-15 (δ_{C} 76.5, d) (Fig. 2), along with seven degrees of unsaturation, permitted assignment of an OAc group at C-15 in **1**. In addition, ROESY correlations (Fig. 3) of H-1/H-5 β /H-9 β , and H-11/H-13 α /H-15 demonstrated that H-1 was β -oriented, while H-11 and H-15 were α -oriented.

To verify the structure of **1**, attempts to crystallize **1** from MeOH were made success and a X-ray diffraction experiment was performed. Single-crystal X-ray diffraction analysis using the anomalous scattering of Cu K α radiation yielded a Flack parameter of 0.01 (14), and a Hoof parameter of 0.03 (3) for 1311 Bijvoet paris, confirming the assignment of absolute configuration of compound **1** to

be 1*S*, 5*R*, 7*R*, 8*S*, 9*S*, 10*R*, 11*S*, 13*S*, 15*R* (Fig. 3). Therefore, the structure of **1** was established as 15 β -acetoxy-7 α ,20-epoxy-1 α ,7 β ,11 β -trihydroxy-*ent*-kaur-16-ene, and it was named 15-acetylmegathyrin B.

Compound **2** was obtained as a white amorphous powder and its molecular formula was determined to be C₂₀H₂₈O₄ by the HRESIMS ([M+Na]⁺ *m/z* 355.1885, calcd 355.1880). Its IR spectrum gave absorption bands at 3482, 1722, and 1641 cm⁻¹, suggesting the presence of hydroxy, carbonyl, and olefinic groups, respectively. In the ¹³C NMR and DEPT spectra (Table 2), 20 carbon signals were observed, which were assigned as two methyls, eight methylenes (one oxygenated and one olefinic), four methines (one oxygenated), and six quaternary carbons (one carbonyl), respectively. Detailed analysis of the NMR data (Tables 1 and 2) indicated that compound **2** was identical to rabdocoestin A (**10**), except for the absence of an OH substituent at C-11 in **2**. The structure of compound **2** was supported by its 2D NMR correlations. The ¹H–¹H COSY correlations of H-1/H₂-2/H₂-3, along with HMBC correlations from H₂-2 (δ_{H} 1.85, 2H, m), H₂-3 (δ_{H} 1.24 and 1.37), H-5 (δ_{H} 1.55), and H-9 (δ_{H} 1.71) to C-1 (δ_{C} 73.7, d), indicated an OH group at C-1. Meanwhile, the HMBC data showed correlations from H-1 (δ_{H} 3.64), H-5 (δ_{H} 1.55), and H-9 (δ_{H} 1.71) to C-20 (δ_{C} 64.3, t), and from H₂-20 (δ_{H} 4.52 and 4.80) to C-7 (δ_{C} 96.1, s), indicating an epoxy ring between C-7 and C-20. Therefore, compound **2** was determined to be a 7 α ,20-epoxy-*ent*-kauranoid. Additionally, ROESY correlations of H-5 β /H-1/H-9 β disclosed a β -orientation of H-1. Thus, the structure of compound **2** was defined as 7 α ,20-epoxy-1 α ,7 β -dihydroxy-*ent*-kaur-16-en-15-one, and it was named serrin E.

Compound **3** was obtained as a white amorphous powder that gave a molecular formula of C₂₀H₂₈O₆ by the HRESIMS ([M-H]⁻ *m/z* 363.1813, calcd 363.1813), implying seven degrees of unsaturation. The NMR data of **3** suggested its structure resembled rabdocoestin A (**10**), except for an OH locating at C-14 in **3**. This was supported by the chemical shift of C-13 ($\Delta\delta$ 9.5 ppm) and C-8 ($\Delta\delta$ 2.5 ppm) in **3** relative to those of **10**. The 2D NMR spectra of **3** further verified that inference: the ¹H–¹H COSY data exhibited H-9/H-11/H-12/H-13/H-14 correlations (Fig. 2), and the HMBC data showed key correlations from H-9 (δ_{H} 2.07), H₂-12 (δ_{H} 2.99, 1.92), and H-13 (δ_{H} 3.27) to C-14 (δ_{C} 73.1, d), confirming an OH group at C-14 (Fig. 2). Furthermore, ROESY correlations of H-5 β /H-1/H-9 β and H-11/H-20 α /H-14 supported configurations of H-1, H-11 and H-14 as being β -, α -, and α -oriented, respectively. Thus, the structure of compound **3** was determined to be 7 α ,20-epoxy-1 α ,7 β ,11 β ,15 β -tetrahydroxy-*ent*-kaur-16-en-15-one, and it was named 14 β -hydroxyrabdocoestin A.

Table 1
¹H NMR spectroscopic data for compounds **1–9** in pyridine-d₅ (δ in ppm, *J* in Hz).

No.	1 ^a	2 ^a	3 ^c	4 ^c	5 ^c	6 ^c	7 ^c	8 ^b	9 ^c
1a	4.21 (dd, 11.2, 5.4)	3.64 (overlap)	4.13 (m)	0.74 (overlap)	4.14 (m)	3.86 (m)	4.87 (overlap)	0.84 (m)	4.86 (dd, 11.5, 5.3)
1b				1.06 (m)				1.12 (m)	
2a	1.90 (2H, m)	1.85 (2H, m)	1.95 (overlap)	1.27 (2H, m)	1.95 (m)	1.9 (2H, m)	1.80 (m)	1.40 (2H, m)	1.82 (2H, m)
2b			1.87 (overlap)		1.86 (m)		1.56 (overlap)		1.50 (overlap)
3a	1.44 (br d, 13.3)	1.37 (dt, 12.5, 4.5)	1.42 (dt, 13.3, 3.2)	1.13 (br d, 13.8)	1.44 (dt, 13.2, 3.1)	1.43 (dt, 13.2, 3.2)	1.32 (br d, 13.5)	1.68 (overlap)	1.34 (br d, 13.3)
3b	1.25 (br t, 12)	1.24 (overlap)	1.24 (dt, 13.5, 3.2)	0.99 (m)	1.26 (dt, 13.6, 3.1)	1.29 (m)	1.19 (br t, 13.7)	1.55 (overlap)	1.24 (br d, 13.3)
5	1.69 (dd, 11.0, 7.6)	1.55 (dd, 11.5, 7.3)	1.59 (dd, 11.5, 6.6)	1.39 (dd, 11.2, 6.9)	1.63 (dd, 11.9, 5.6)	1.60 (m)	1.60 (overlap)	2.07 (overlap)	1.66 (m)
6a	2.13 (overlap)	3.67 (overlap)	3.74 (br t, 12.7)	3.56 (m)	3.52 (br t, 12.5)	2.16 (dd, 12.2, 7.6)	3.49 (t, 12.4)	3.65 (t, 12.2)	2.12 (t, 12.5)
6b	2.03 (overlap)	2.04 (dd, 12.9, 7.3)	2.05 (overlap)	1.99 (dd, 13.4, 6.9)	2.01 (dd, 12.5, 5.6)	3.78 (t, 12.2)	2.01 (overlap)	2.13 (overlap)	2.00 (overlap)
9	2.47 (d, 10.1)	1.71 (dd, 12.9, 5.5)	2.07 (overlap)	1.61 (overlap)	1.81 (overlap)	1.57 (d, 3.4)	1.75 (overlap)	1.61 (overlap)	2.45 (dd, 13.1, 5.9)
11a	4.67 (m)	2.43 (m)	4.91 (overlap)	1.58 (overlap)	4.79 (m)	4.58 (m)	2.38 (m)	1.64 (overlap)	1.90 (m)
11b		1.96 (m)		1.13 (m)			1.43 (m)		1.18 (m)
12a	2.85 (m)	2.23 (m)	2.99 (m)	2.32 (m)	2.48 (overlap)	1.79 (dd, 15.0, 5.3)	2.19 (2H, m)	2.34 (m)	2.33 (m)
12b	1.83 (overlap)	1.41 (overlap)	1.92 (overlap)	1.51 (m)	1.82 (overlap)	2.66 (dd, 15.0, 9.7)		1.50 (overlap)	1.56 (m)
13a	2.68 (m)	2.88 (dd, 9.6, 3.8)	3.27 (br d, 10.0)	3.10 (br d, 9.6)	2.81 (m)	3.13 (dd, 4.2, 9.7)		3.11 (br d, 9.6)	2.80 (br d, 9.2)
14a	2.09 (2H, overlap)	2.46 (br d, 12.2)	5.46 (H, s)	5.17 (s)	2.43 (dd, 12.5, 3.3)	3.69 (dd, 11.5)	2.86 (2H, m)	5.19 (s)	5.04 (s)
14b		2.38 (dd, 12.2, 3.8)			2.51 (overlap)	2.52 (dd, 11.5, 4.3)			
15	6.35 (s)								6.85 (s)
16					2.94 (m)		3.10 (t, 4.8)		
17a	5.12 (2H, br s)	6.00 (s)	6.29 (s)	6.27 (s)	3.88 (dd, 10.3, 4.6)	6.02 (s)	3.98 (2H, m)	6.26 (s)	5.33 (s)
17b		5.23 (s)	5.46 (s)	5.41 (s)	3.71 (dd, 10.3, 4.6)	5.25 (s)		5.42 (s)	5.25 (s)
18	0.77 (3H, s)	0.79 (3H, s)	0.78 (3H, s)	0.76 (3H, s, overlap)	0.75 (3H, s)	0.83 (3H, s)	0.72 (3H, s)	3.63 (d, 10.6)	0.77 (3H, s)
18b								3.54 (2H, d, 10.6)	
19	1.08 (3H, s)	1.11 (3H, s)	1.13 (3H, s)	1.03 (3H, s)	1.12 (3H, s)	1.12 (3H, s)	1.06 (3H, s)	1.15 (3H, s)	1.05 (3H, s)
20a	4.81 (d, 10.0)	4.80 (d, 10.0)	4.87 (overlap)	4.29 (d, 9.9)	4.75 (d, 10.3)	5.29 (2H, dd, 9.4)	4.54 (d, 10.1)	4.39 (d, 9.8)	4.57 (d, 9.9)
20b	4.57 (d, 10.0)	4.52 (d, 10.0)	4.67 (dd, 10.3, 1.8)	3.98 (d, 9.9)	4.61 (d, 10.3)	1.7)	4.43 (d, 10.1)	4.06 (d, 9.8)	4.45 (d, 9.9)
OAc-1							2.03 (3H, s)		2.03 (3H, s)
OAc-15	2.16 (3H, s)								2.28 (3H, s)
OMe					3.22 (3H, s)		3.3 (3H, s)		

^a Recorded at 400 MHz.

^b Recorded at 500 MHz.

^c Recorded at 600 MHz.

Compound **4** was obtained as a white amorphous powder, and it had a molecular formula C₂₀H₂₈O₄ as deduced from the HRESIMS ([M+H]⁺ *m/z* 333.2062, calcd 333.2060), including seven degrees of unsaturation. The NMR spectroscopic data of **4** were similar to those of longikaurin A (**17**) (Fig. 1) (Fujita et al., 1980), except for the absence of an oxygenated carbon (δ_C 64.5, d) and the presence of one more methylene (δ_C 32.2, t) in **4**. The position of the OH substituent in **4** was deduced by the ¹H–¹H COSY and HMBC correlations. The ¹H–¹H COSY correlations of H₂-11/H₂-12/H₂-13/H-14 and HMBC correlations from H-9 (δ_H 1.61), H₂-12 (δ_H 1.51, 2.32), and H-13 (δ_H 3.10) to C-14 (δ_C 73.2, d) indicated an OH group at C-14. The configuration of H-14 was established as α -oriented due to the correlation between H-20 with H-14 in its ROESY spectrum. Compound **4** was then established as 7 α ,20-epoxy-7 β ,14 β -dihydroxy-ent-kaur-16-en-15-one, and it was named serrin F.

Compound **5** possessed a molecular formula of C₂₁H₃₂O₆, corresponding to its molecular ion peak *m/z* 379.2127 ([M-H]⁻, calcd 379.2126), implying six degrees of unsaturation. The NMR data of **5** resembled those of nervosanin A (**18**) (Fig. 1) (Wang et al., 1994) except for one OH group at C-11 in **5** relative to C-6 in nervosanin A. The ¹H–¹H COSY correlations of H-9/H-11/H-12/H-13/H-14, as well

as HMBC correlations from H-9 (δ_H 1.81), H₂-12 (δ_H 1.82, 2.48), and H-13 (δ_H 2.81) to C-11 (δ_C 63.9, d), confirmed a hydroxy substituent at C-17 in **5**. The β -orientation of H-1, H-11, and MeO-17 were determined by the ROESY correlations of H-1/H-5 β /H-9 β , H-11/H-1 and H-17/H-9 β , respectively. Consequently, compound **5** was assigned as 7 α ,20-epoxy-1 α ,7 β ,11 α -trihydroxy-17 β -methoxy-ent-kaur-15-one, and it was named serrin G.

Compound **6** was obtained as a white amorphous powder and it had a same overall structure as rabdocoestin A (**10**) according to the HRESIMS ([M-H]⁻, *m/z* 347.1865; calcd 347.1864) and NMR spectra (Tables 1 and 2). The ¹³C NMR spectroscopic data showed chemical shifts of C-9 ($\Delta\delta$ 2.2 ppm) and C-11 ($\Delta\delta$ 4.2 ppm) in **6** compared to those of **10**, which might be caused by the inverse orientation of OH-11 in **6**. The ROESY correlations of H-11/H-1 β /H-9 β verified the β -orientation of H-11 in **6**. Thus, **6** was assigned to be 7 α ,20-epoxy-1 α ,7 β ,11 α -trihydroxy-ent-kaur-16-en-15-one, and it was named 11-*epi*-rabdocoestin A.

Compound **7** was obtained as a white amorphous powder and its molecular formula was established to be C₂₃H₃₄O₇ by the HREIMS ([M]⁺ *m/z* 422.2284, calcd 422.2305). Comparisons of the ¹H and ¹³C NMR spectroscopic data of **7** with those of lasiokaurinin

Table 2
 ^{13}C NMR spectroscopic data for compounds **1–9** in pyridine- d_5 (δ in ppm).

Position	1 ^a	2 ^a	3 ^c	4 ^c	5 ^c	6 ^c	7 ^c	8 ^b	9 ^c
1	73.8 d	73.7 d	73.8 d	30.5 t	74.1 d	73.9 d	76.6 d	30.9 t	76.9 d
2	28.4 t	30.5 t	28.9 t	18.8 t	28.6 t	29.8 t	25.7 t	18.6 t	25.9 t
3	39.5 t	39.1 t	39.7 t	40.8 t	39.9 t	39.2 t	38.6 t	35.2 t	38.6 t
4	34.2 s	34.0 s	34.7 s	33.8 s	34.6 s	34.4 s	34.1 s	35.9 s	34.1 s
5	48.3 d	49.2 d	48.6 d	48.7 d	49.5 d	50.1 d	49.9 d	42.8 d	49.0 d
6	34.5 t	33.1 t	32.9 t	32.2 t	32.9 t	33.7 t	33.6 t	32.3 t	34.6 t
7	95.4 s	96.1 s	98.8 s	98.1 s	96.5 s	96.9 s	96.2 s	98.2 s	98.5 s
8	53.6 s	57.9 s	59.9 s	59.5 s	59.1 s	57.6 s	61.3 s	59.7 s	53.8 s
9	52.5 d	52.0 d	60.0 d	52.3 d	58.7 d	55.3 d	50.3 d	52.4 d	48.0 d
10	41.3 s	41.2 s	42.5 s	35.9 s	42.3 s	43.1 s	39.8 s	39.0 s	39.2 s
11	63.0 d	20.4 t	62.4 d	16.4 t	63.9 d	67.6 d	20.7 t	16.6 t	17.3 t
12	42.7 t	30.7 t	40.5 t	30.6 t	31.1 t	40.2 t	32.3 t	30.7 t	33.3 t
13	37.1 d	34.5 d	43.8 d	43.0 d	29.8 d	34.6 d	74.5 s	43.2 d	46.2 d
14	27.1 t	25.8 t	73.1 d	73.2 d	28.9 t	27.0 t	37.1 t	73.4 d	75.3 d
15	76.5 d	205.7 s	204.5 s	203.6 s	218.4 s	206.5 s	216.5 s	203.7 s	75.5 d
16	158.6 s	155.3 s	153.9 s	153.6 s	58.6 d	155.6 s	63.7 d	153.7 s	158.0 s
17	108.5 t	113.5 t	117.3 t	116.9 t	70.0 t	113.4 t	69.3 t	117.0 t	111.3 t
18	32.0 q	31.8 q	32.2 q	32.2 q	32.3 q	32.5 q	31.8 q	70.8 t	32.1 q
19	21.2 q	20.7 q	21.4 q	20.7 q	21.3 q	21.3 q	20.7 q	17.1 q	21.0 q
20	64.6 t	64.3 t	65.4 t	66.3 t	65.6 t	66.6 t	64.3 t	67.2 t	63.9 t
OAc-1							170.6 s		107.6 s
							21.8 q		21.9 q
OAc-15	170.7 s								171.3 s
	21.3 q								21.8 q
OMe					59.1 q		59.2 q		

^a Recorded at 100 MHz.

^b Recorded at 125 MHz.

^c Recorded at 150 MHz.

(**19**) (Fig. 1) (Fujita et al., 1974) indicated that both compounds had an identical skeleton and groups, only differing in an OH group at C-13 in **7** instead of C-6 and C-14. This conclusion was confirmed by the key HMBC correlations from H₂-12 (δ_{H} 2.19, 2H, m), H₂-14 (δ_{H} 2.86, 2H, m), and H-16 (δ_{H} 3.10) to C-13 (δ_{C} 74.5, s) (Fig. 2). The stereogenic carbons were accordingly assigned as H-1 β , HO-13 α and H-16 α , respectively, based on ROESY correlations of H-1/H-5 β /H-9 β and H₂-17/H-9 β . The structure of **7** was determined to be 1 α -acetoxy-7 α ,20-epoxy-7 β ,13 α -dihydroxy-17 β -methoxy-*ent*-kaur-15-one, and it was named serrin H. It was the first example of *ent*-kauranoid bearing an oxy-13 and oxy-17 moiety in D-ring isolated from *Isodon* species.

Compound **8** obtained as a white amorphous powder displayed a molecular ion peak at m/z 348.2013, in accordance with its molecular formula of C₂₀H₂₈O₅. The ^{13}C NMR and DEPT spectra

suggested that **8** was a 7,20-epoxy-*ent*-kauranoid with one more hydroxy group at C-18 compared to serrin H (**4**). HMBC correlations from H₂-3 (δ_{H} 1.68, 1.55), H-5 (δ_{H} 2.07), and CH₃-19 (δ_{H} 1.15, 3H, s) to C-18 (δ_{C} 70.8, t) (Fig. 2), along with the up-field shift of C-5 ($\Delta\delta$ 5.9 ppm) due to the γ -gauche steric compression effect, confirmed an OH-18 fragment in **8**. The ROESY spectra of **8** indicated that the relative configurations of its stereogenic carbons were identical to those of **4**. Therefore, **8** was identified as 7 α ,20-epoxy-7 β ,14 β ,18-trihydroxy-*ent*-kaur-16-en-15-one, and it was named serrin I.

Compound **9** was obtained as a white amorphous powder that gave a molecular formula of C₂₄H₃₄O₇ by the HRESIMS ([M+Na]⁺ m/z 457.2198, calcd 457.2197). It possessed a somewhat analogous structure compared to rabdocoestin B (**11**), except for an acetoxy group at C-15 in **9** instead of a carbonyl group in **11**. This was verified by HMBC correlations from H-14 (δ_{H} 5.04), H₂-17 (δ_{H} 5.25, 5.33), and CH₃-OAc (δ_{H} 2.28, 3H, s) to C-15 (δ_{C} 75.5, d). The orientations of the substituents were assigned to be AcO-1 α , HO-14 β , and AcO-15 β , respectively, based on ROESY correlations of H-1/H-5 β /H-9 β , H-14/H-20b, and H-15/H-13 α . Accordingly, the structure of **9** was determined to be 1 α ,15 β -diacetoxy-7 α ,20-epoxy-7 β ,14 β -dihydroxy-*ent*-kaur-16-en-15-one, and it was named to be 15-acetylanenderianin N.

The known compounds **10–16** were identified by the comparisons of their spectroscopic data with those reported in the literatures.

According to the cytotoxic activities of those diterpenoids isolated from *I. serra* previously, all isolates in this study were submitted to testing for their *in vitro* cytotoxicity against five human tumor cell lines (HL-60, SMMC-7721, A-549, MCF-7, SW-480) using the MTS method (Monks et al., 1991), with *cis*-platin and paclitaxel as positive controls. Compounds **4**, **11** and **13** exhibited weak cytotoxicity to all human tumor cell lines, with IC₅₀ values ranging from 0.7 to 4.6 μM , compared with paclitaxel (IC₅₀ values ranging from 0.09×10^{-3} to 0.89×10^{-3} μM), whereas compounds **2**, **6**, **10**, **11**, **14** and **15** showed even lower activities towards all five (Table 3).

Inflammation is a systemic response aimed to decrease the

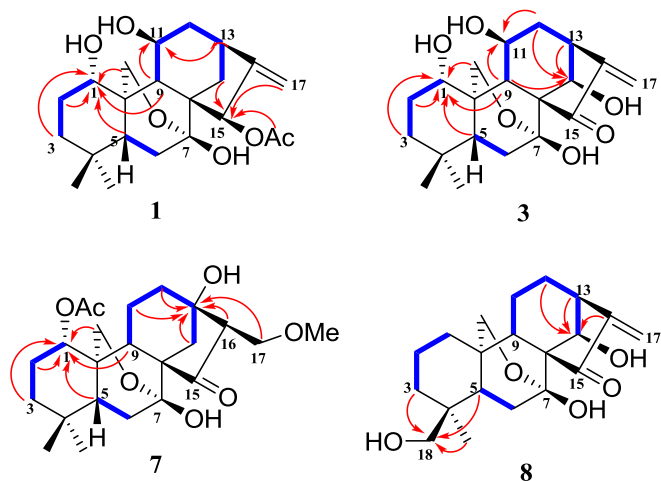


Fig. 2. Selected HMBC (arrows) and ^1H - ^1H COSY (bold) correlations of **1**, **3**, **7** and **8**.

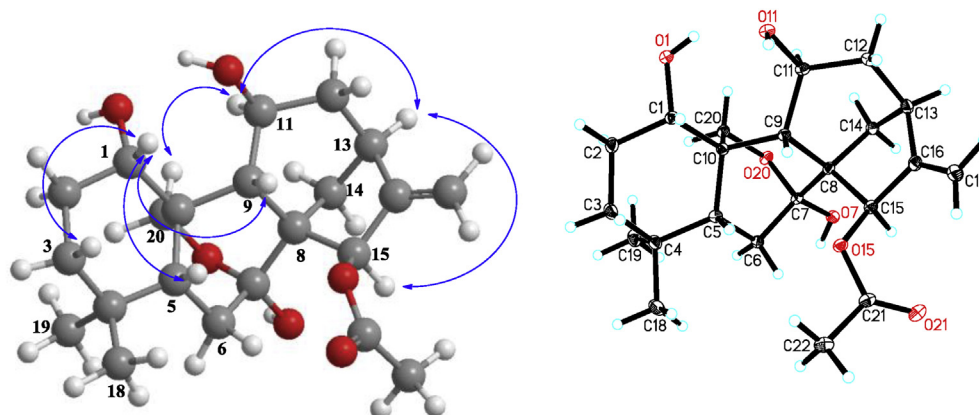


Fig. 3. Key ROESY correlations and X-ray crystallographic structure of compound 1.

Table 3

Cytotoxic activities of several diterpenoids from *Isodon serra* against tumor cell lines, IC₅₀ values (μM).

Compounds ^a	HL-60	SMMC-7721	A-549	MCF-7	SW480
2	3.6	>10	>10	4.1	4.1
4	0.7	2.3	3.7	2.2	3.4
6	5.3	9.5	>10	5.3	6.6
10	3.3	4.3	>10	4.1	3.3
11	2.7	1.4	4.6	2.4	2.2
13	0.8	1.7	4.4	2.4	2.6
14	5.0	8.2	>10	6.2	7.3
15	2.7	3.0	>10	3.1	2.1
DDP ^b	1.9	11.8	12.4	18.3	18.1
Paclitaxel ^b	0.09 × 10 ⁻³	0.64 × 10 ⁻³	0.89 × 10 ⁻³	0.37 × 10 ⁻³	0.72 × 10 ⁻³

^a Compounds **1**, **3**, **5**, **7**, **8**, **9**, **12** and **16** had IC₅₀ > 10 μM for all cell lines.

^b DDP (*cis*-platin) and paclitaxel were used as positive controls.

toxicity of harmful agents and repair damaged tissue. A key feature of the inflammatory response is the activation of phagocytic cells involved in host defense. NO, a free radical produced by the inducible NO synthase (iNOS) isoform, is an essential component of the host innate immune and inflammatory responses to a variety of pathogens (McCartney-Francis et al., 2001). Due to the widespread folk use of *I. serra* for curing hepatitis and cholecystitis, all isolates except compounds **1** and **9** were tested for their inhibitory activities against NO production in LPS-stimulated RAW264.7 cells using the MTS assay. The experimental results showed that most compounds exhibited significant NO inhibitory effects: compound **4** exhibited a remarkable NO inhibitory effect with an IC₅₀ value of 0.6 μM, while compounds **2**, **11**, **13** and **14** exhibited potent active effects with IC₅₀ values of 1.4, 1.4, 1.3 and 1.5 μM, respectively (Table 4). Compounds **3**, **7**, **8**, **12** and **16** also exhibited inhibitory effects towards NO production, while no cytotoxicity against five cell lines was detected (IC₅₀ > 10 μM).

3. Concluding remarks

Ent-kaurane diterpenoids are the primary chemical constituents of *Isodon* species responsible for the bioactivities of the plants (Wang et al., 2012; Wu et al., 2014; Yang et al., 2016), and the studies herein on *I. serra* added nine new ones. Among the isolates, two compounds exhibited weak cytotoxicity compared with paclitaxel, as well as a new one that showed remarkable effect against NO production. To some extent, the above bioactivity results gave a preliminary foundation for the interpretation of the folk effect of this species.

Table 4

Inhibitory effects of compounds **2–4**, **6–8** and **10–16** on LPS-stimulated NO production in RAW264.7 cells.^a

Compounds	IC ₅₀ (μM)	Compounds	IC ₅₀ (μM)
2	1.4	11	1.4
3	7.6	12	3.9
4	0.6	13	1.3
6	2.1	14	1.5
7	5.9	15	2.1
8	4.6	16	2.8
10	2.0	MG-132 ^b	0.2

^a Each value represents the mean ± SEM (n = 3).

^b Positive control.

4. Experiments

4.1. General experimental procedures

X-ray data were collected using a Bruker APEX instrument. Optical rotations were measured in MeOH on a JASCO P-1020 digital Polarimeter, whereas UV spectra data were obtained on a Shimadzu UV2401PC spectrophotometer. A tensor 27 spectrophotometer was used for scanning IR spectroscopy with KBr pellets. 1D- and 2D-NMR (δ_{H} 8.71, 7.55 and 7.19 for pyridine-d₅) spectra were recorded on Bruker AM-400, DRX-500 and DRX-600 spectrometers. Unless otherwise specified, chemical shifts (δ) were expressed in ppm with reference to the solvent signals. HRESIMS was performed on a VG Autospec-3000 spectrometer at 70 eV. HREIMS was performed on a VG Autospec-Premier P776 at 70 eV. Column chromatography (CC) was performed with silica gel

(100–200 mesh; Qingdao Marine Chemical, Inc., Qingdao, People's Republic of China). Semipreparative HPLC was performed on an Agilent 1100 and Agilent 1200 liquid chromatograph with a Zorbax SB-C₁₈ (9.4 mm × 25 cm) column. Preparative HPLC was performed on an Agilent 1260 liquid chromatograph with a Zorbax SB-C₁₈, 21 mm × 25 cm column. MCI gel (75–150 μm, Mitsubishi Chemical Corporation, Tokyo, Japan), and Sephadex LH-20 gel (40–70 μm, Amersham Pharmacia Biotech AB, Uppsala, Sweden), respectively. Lichroprep RP-18 gel (40–63 μm), Merck, Darmstadt, Germany. Fractions were monitored by TLC and spots were visualized by heating silica gel plates sprayed with 5% H₂SO₄ in EtOH. All solvents including petroleum ether were distilled prior to use.

4.2. Plant material

The aerial parts of *I. serra* were collected in E'mei Mountain, Sichuan Province, People's Republic of China, in August 2008. The voucher specimen (KIB 2008091703) is deposited at the State Key Laboratory of Phytochemistry and Plant Resources in West China, Kunming Institute of Botany, Chinese Academy of Sciences, and identified by Prof. Xi-Wen Li.

4.3. Extraction and isolation

Air-dried aerial parts (6 kg) of *I. serra* were powdered and extracted with acetone–H₂O (3 × 20 L, 70:30, v/v, each for 3 days) at room temperature to give a crude extract. The extracts were combined and concentrated to about 2 L and then extracted with EtOAc (5 × 2 L), resulting in EtOAc soluble (ca. 300 g). This portion was then subjected to silica gel CC (1 kg, 100–200 mesh), eluting with CHCl₃–Me₂CO (1:0–0:1 gradient system) to produce seven fractions (Fr. 1–7). Each fraction was then decolorized on MCI gel, eluted with MeOH–H₂O (90:10, v/v).

Fr. 3 (37 g) was subjected to RP-18 CC (eluted with a MeOH–H₂O gradient 30:70–100:0) to give subfractions 3A–3H. Fr. 3F (1.0 g) was applied to preparative HPLC (CH₃CN–H₂O, 30:70 v/v) and then semi-preparative HPLC (CH₃CN–H₂O, 25:75 v/v) to give **3** (6.7 mg), **4** (5.0 mg) and **13** (6.6 mg). Due to the low solubility of the main component of **10**, Fr. 3E (30 g) was washed with MeOH repeatedly to give a pure white powder (10 g), and the corresponding solution (named Fr. 3Ea). Fr. 3Ea (8.436 g) was separated by silica gel, eluting with CHCl₃–Me₂CO (1:0–0:1 gradient system) to produce six portions (3Ea1–3Ea6). Fr. 3Ea3 (1.85 g) was applied to a RP-18 column, eluted with MeOH–H₂O (45:55–80:20 v/v) and by semi-preparative HPLC (CH₃CN–H₂O, 30:70 v/v) to give **5** (3 mg), **14** (8.3 mg), **15** (2 mg), respectively. Fr. 3Ea4 (2.58 g) was subjected to silica gel CC, eluting with CHCl₃–Me₂CO (1:0–0:1 gradient) and then one subfraction (83.5 mg) was applied to preparative TLC (petroleum ether–Me₂CO, 20:1 v/v) and to semipreparative HPLC (CH₃CN–H₂O, 30:70 v/v) to yield **2** (48.4 mg) and **12** (8.7 mg). Fr. 3Ea5 (2.73 g) was subjected to RP-18 CC with MeOH–H₂O (45:55–80:20 gradient), preparative HPLC (CH₃CN–H₂O, 35:65 v/v) and semipreparative HPLC (CH₃CN–H₂O, 28:72 v/v) to yield **1** (11 mg), **6** (3.7 mg) and **7** (3.5 mg). Fr. 2 (14 g) was washed repeatedly to yield **11** (8.0 g), with the wash solution subjected to RP-18 CC (MeOH–H₂O, 50:50–90:10 v/v) and then semi-preparative HPLC (CH₃CN–H₂O, 38:62 v/v) to afford **9** (12.6 mg), **8** (40 mg) and **16** (100 mg) were isolated from Fr. 4 (16 g) by silica gel (petroleum ether–Me₂CO, 30:1–0:1 gradient system), Sephadex LH-20 gel CC (CHCl₃–MeOH, 1:1 v/v) and preparative HPLC (MeOH–H₂O, 32:68 v/v).

4.3.1. 15-Acetylmegathyrin B (1)

Colorless needles; [α]_D²⁰ –62 (c 0.12, MeOH); UV (MeOH) λ_{max} nm (log ε): 201 (3.07), 254 (2.61); IR (KBr) ν_{max} 3355, 2941, 1744,

1632, 1369, 1233, 1050, 921 cm⁻¹; For ¹H and ¹³C NMR spectroscopic data, see Tables 1 and 2; HRESIMS (positive-ion mode) *m/z* 415.2093 [M+Na]⁺ (calcd for C₂₂H₃₂O₆Na, 415.2091).

4.3.2. Serrin E (2)

White amorphous powder; [α]_D²⁰ –108 (c 0.18, MeOH); UV (MeOH) λ_{max} nm (log ε) 234 (3.17), 343 (1.22); IR (KBr) ν_{max} 3482, 2951, 2863, 1722, 1641, 1364, 1167, 1057, 925 cm⁻¹; For ¹H and ¹³C NMR spectroscopic data, see Tables 1 and 2; HRESIMS (positive-ion mode) *m/z* 355.1885 [M+Na]⁺ (calcd for C₂₀H₂₈O₄Na, 355.1880).

4.3.3. 14β-Hydroxyrabdocoestins A (3)

White amorphous powder; [α]_D²⁵ –66 (c 0.10, MeOH); UV (MeOH) λ_{max} nm (log ε) 196 (2.81), 230 (3.15); IR (KBr) ν_{max} 3423, 2937, 2872, 1723, 1642, 1384, 1159, 1062, 968 cm⁻¹; For ¹H and ¹³C NMR spectroscopic data, see Tables 1 and 2; HRESIMS (negative-ion mode) *m/z* 363.1813 [M-H]⁻ (calcd for C₂₀H₂₇O₆, 363.1813).

4.3.4. Serrin F (4)

White amorphous powder; [α]_D²⁵ –100 (c 0.06, MeOH); UV (MeOH) λ_{max} nm (log ε) 229 (3.18), 334 (1.22); IR (KBr) ν_{max} 3420, 2927, 2869, 1727, 1645, 1477, 1273, 1169, 1059, 894 cm⁻¹; For ¹H and ¹³C NMR spectroscopic data, see Tables 1 and 2; HRESIMS (positive-ion mode) *m/z* 333.2062 [M+H]⁺ (calcd for C₂₀H₂₉O₄, 333.2060).

4.3.5. Serrin G (5)

White amorphous powder; [α]_D²⁵ –84 (c 0.07, MeOH); UV (MeOH) λ_{max} nm (log ε) 202 (2.44), 373 (0.93); IR (KBr) ν_{max} 3431, 2933, 2872, 1732, 1385, 1631, 1162, 1062, 612 cm⁻¹; For ¹H and ¹³C NMR spectroscopic data, see Tables 1 and 2; HRESIMS (negative-ion mode) *m/z* 379.2127 [M-H]⁻ (calcd for C₂₁H₃₁O₆, 379.2126).

4.3.6. 11-epi-Rabdocoestins A (6)

White amorphous powder; [α]_D²⁵ –118 (c 0.14, MeOH); UV (MeOH) λ_{max} nm (log ε) 232 (3.17); IR (KBr) ν_{max} 3423, 2929, 1718, 1642, 1384, 1269, 1163, 1053, 921 cm⁻¹; For ¹H and ¹³C NMR spectroscopic data, see Tables 1 and 2; ESIMS (negative-ion mode) *m/z* 347.1865 [M-H]⁻ (calcd for C₂₀H₂₇O₅, 347.1864).

4.3.7. Serrin H (7)

White amorphous powder; [α]_D²⁶ –82 (c 0.10, MeOH); UV (MeOH) λ_{max} nm (log ε) 228 (3.05); IR (KBr) ν_{max} 3438, 2926, 2876, 1688, 1630, 1443, 1384, 1263, 1091, 1015 cm⁻¹; For ¹H and ¹³C NMR spectroscopic data, see Tables 1 and 2; HRESIMS (positive-ion mode) *m/z* 422.2284 [M]⁺ (calcd for C₂₃H₃₄O₇, 422.2305).

4.3.8. Serrin I (8)

White amorphous powder; [α]_D²³ –70 (c 0.18, MeOH); UV (MeOH) λ_{max} nm (log ε) 199 (2.73), 229 (3.00); IR (KBr) ν_{max} 3425, 2931, 2867, 1727, 1643, 1446, 1384, 1273, 1174, 1057, 893 cm⁻¹; For ¹H and ¹³C NMR spectroscopic data, see Tables 1 and 2; HRESIMS (positive-ion mode) *m/z* 349.2013 [M+H]⁺ (calcd for C₂₀H₂₉O₅, 349.2010).

4.3.9. 15-Acetylenanderianin N (9)

White amorphous powder; [α]_D²³ –45 (c 0.10, MeOH); UV (MeOH) λ_{max} (log ε) nm 201 (2.96), 254 (2.31), 321 (1.43); IR (KBr) ν_{max} 3435, 2952, 2869, 1739, 1631, 1405, 1373, 1241, 1173, 1045, 603 cm⁻¹; For ¹H and ¹³C NMR spectroscopic data, see Tables 1 and 2; HRESIMS (positive-ion mode) *m/z* 457.2198 [M+Na]⁺ (calcd for C₂₄H₃₄O₇Na, 457.2197).

4.4. X-ray crystal structure analysis

Colorless crystals of **1** were obtained in MeOH. Intensity data

were collected at 100 k on a Bruker APEX DUO diffractometer equipped with an APEX II CCD, using Cu K α radiation. Cell refinement and data reduction were performed with Bruker SAINT. The structures were solved by direct methods using SHELXS-97 (Sheldrick and Schneider, 1997). Refinements were performed with SHELXL-97 using full-matrix least-squares, with anisotropic displacement parameters used for all the non-hydrogen atoms. The H atoms were placed in the calculated positions and refined using a riding model. Molecular graphics were computed with PLATON. Crystallographic data (excluding structure factor tables) for the structures reported have been deposited with the Cambridge Crystallographic Data Center as supplementary publication no. CCDC 1443993 for **1**. Copies of the data can be obtained free of charge on application to CCDC, 12 Union Road, Cambridge CB 1EZ, UK [fax: Int. + 44 (0) (1223) 336 033; e-mail: deposi@ccdc.cam.ac.uk].

4.5. Crystallographic data for 15-acetylmegathyrin B (**1**)

C₂₂H₃₂O₆, $M_w = 392.48$, tetragonal, space group, P43212, $Z = 8$, $a = 11.1115(2) \text{ \AA}$, $b = 11.1115(2) \text{ \AA}$, $c = 31.8353(5) \text{ \AA}$; $\alpha = \beta = \gamma = 90^\circ$, $V = 3930.56(12) \text{ \AA}^3$, $T = 100(2) \text{ K}$, $\mu (\text{Cu K}\alpha) = 0.778 \text{ mm}^{-1}$, 21,872 reflections measured, 3457 independent reflections ($R_{int} = 0.0355$). The final R_1 values were 0.0288 [$I > 2\sigma(I)$]. The final $wR_2 (F^2)$ values were 0.0746 [$I > 2\sigma(I)$]. The final R_1 values were 0.0289 (all data). The final $wR_2 (F^2)$ values were 0.0746 (all data). The goodness of fit on F^2 was 1.095. Flack parameter = 0.01(14). The Hooft parameter is 0.03(3) for 1311 Bijvoet pairs.

4.6. Cytotoxicity assays

The human tumor cell lines HL-60, SMMC-7721, A-549, MCF-7, and SW-480 were used, which were obtained from ATCC (Manassas, VA, USA). All cells were cultured in RPMI-1640 or DMEM medium (Hyclone, Logan, UT, USA), supplemented with 10% fetal bovine serum (Hyclone) at 37 °C in a humidified atmosphere with 5% CO₂. Cell viability was assessed by conducting colorimetric measurements of the amount of insoluble formazan formed in living cells based on the reduction of MTS (Sigma, St. Louis, MO, USA) (Monks et al., 1991). Briefly, adherent cells (100 μL) were seeded into each well of a 96-well cell culture plate and allowed to adhere for 12 h before test compound addition, while suspended cells were seeded just before test compound addition, both with an initial density of 1×10^5 cells/mL in 100 μL of 20% SDS-50% DMF after removal of 100 μL of medium. The optical density of the lysate was measured at 595 nm in a 96-well microtiter plate reader (Bio-Rad 680). The IC₅₀ value of each compound was calculated by Reed and Muench's method (Reed and Muench, 1938).

4.7. Nitric oxide production in RAW 264.7 macrophages

Murine monocytic RAW264.7 macrophages were dispensed into 96-well plates (2×10^5 cells/well) containing RPMI 1640 medium (Hyclone) with 10% FBS under a humidified atmosphere of 5% CO₂ at 37 °C. After 24 h pre-incubation, cells were treated with serial dilutions of the presence of 1 $\mu\text{g}/\text{mL}$ LPS for 18 h. Each compound was dissolved in DMSO and further diluted in medium to produce different concentrations. NO production in each well was assessed by adding 100 μL of Griess reagent (reagent A and reagent B, respectively, Sigma) to 100 μL of each supernatant from LPS (Sigma)-treated or LPS- and compound-treated cells in triplicate. After 5 min incubation, the absorbance was measured at 570 nm with a 2104 Envision multitablet plate reader (Perkin-Elmer Life Sciences, Inc., Boston, MA, USA). MG-132 was used as a positive control (Fan et al., 2010).

4.8. Determination of cytotoxic effects

The cytotoxicity of tested compounds was evaluated using an MTS assay (Monks et al., 1991). Briefly, RAW264.7 cells, 2×10^5 cells/well, were seeded in 96-well plates. After 24 h incubation, cells were treated with or without test compounds at given concentrations for 18 h. Then, MTS was added to each well and the plates were kept for 4 h. Testing compounds were dissolved in DMSO, and the absorbance was read at 490 nm. Cytotoxicity was calculated by cell viability of cells without compounds as 100%.

Acknowledgments

This project was supported financially by the NSFC-Joint Foundation of Yunnan Province (Grant U1302223), the National Natural Science Foundation of China (Grants 21322204 and 21402213), and the West Light Foundation of the Chinese Academy of Sciences (J.-X. Pu).

Appendix A. Supplementary data

Supplementary data related to this article can be found at <http://dx.doi.org/10.1016/j.phytochem.2016.05.014>.

References

- Chen, Y.P., Sun, H.D., Lin, Z.W., 1990. Study on the diterpenoids of *Rabdosia coetsa*. *Acta Bot. Sin.* 32, 292–296.
- Du, Y.F., Liu, P.W., Zhu, H., Shi, X.W., Zhao, C.C., Wang, N., Zhang, L.T., 2011. A sensitive analysis method for 7 diterpenoids in rat plasma by liquid chromatography-electrospray ionization mass spectrometry and its application to pharmacokinetic study of *Isodon serra* extract. *J. Chromatogr. A* 1218, 7771–7780.
- Fan, J.T., Su, J., Peng, Y.M., Li, Y., Li, J., Zhou, Y.B., Zeng, G.Z., Yan, H., Tan, N.H., 2010. Rubiyunnanins C-H, cytotoxic cyclic hexapeptides from *Rubia yunnanensis* inhibiting nitric oxide production and NF- κ B activation. *Bioorg. Med. Chem.* 18, 8226–8234.
- Flora of China, 1977. Science Press, Beijing, p. 433.
- Fujita, E., Taoka, M., Fujita, T., 1974. Terpenoids. XXVI. Structures of lasiokaurinol and lasiokaurinin, two novel diterpenoids of *Isodon lasiocarpus*. *Chem. Pharm. Bull.* 22, 280–285.
- Fujita, T., Takeda, Y., Shingu, T., 1980. Longikaurin A and B; new, biologically active diterpenoids from *Rabdosia longituba*. *J. Chem. Soc. Chem. Commun.* 5, 205–207.
- Fukita, E., Fujita, T., Fuji, K., Ito, N., 1965. The absolute configuration of enmein. Transformation of enmein into (-)-kaurane. *Chem. Pharm. Bull.* 13, 1023–1027.
- Hai, G.F., Niu, B.X., Bai, S.P., Liu, J.Y., 2010. Effect of radoserrin B on cell growth of human retinoblastoma. *Rec. Adv. Ophthalmol.* 30, 332–334.
- Iitaka, Y., Natsume, M., 1964. The x-ray study of acetyl bromoacetyl dihydroenmein. *Tetrahedron Lett.* 1257–1261.
- Ikeda, T., Kanamoto, S., 1958. Bitter principles of *Isodon trichocarpus* (*Plectranthus trichocarpus*). *J. Yakugaku Zasshi* 78, 1128–1132.
- Jin, R.L., Cheng, P.Y., Xu, G.Y., 1985. The structure of radoserrin A, isolated from *Rabdosia serra* (Maxim) Hara. *Acta Pharm. Sin.* 20, 366–371.
- Jin, R.L., Cheng, P.Y., Xu, G.Y., 1987. Structure of radoserrin B, isolated from *Rabdosia serra*. *J. Chin. Pharm. Univ.* 18, 172–174.
- McCartney-Francis, N.L., Song, X.Y., Mizel, D.E., Wahl, S.M., 2001. Selective inhibition of inducible nitric oxide synthase exacerbates erosive joint disease. *J. Immunol.* 166, 2734–2740.
- Monks, A., Scudiero, D., Skehan, P., Shoemaker, R., Paull, K., Vistica, D., Hose, C., Langley, J., Cronise, P., Vaigro-Wolf, A., 1991. Feasibility of a high-flux anticancer drug screen using a diverse panel of cultured human tumor cell lines. *J. Natl. Cancer Inst.* 83, 757–766.
- Qiu, S.X., Sun, H.D., Lobkovsky, E., Chai, H.Y., Clardy, J., Farnsworth, N.R., Pezzuto, J.M., Fong, H.S., 1998. A cytotoxic diterpene from *Isodon megathyrus*. *Planta Med.* 64, 728–731.
- Reed, L.J., Muench, H., 1938. A simple method of estimating fifty percent endpoints. *Am. J. Hyg.* 27, 493–497.
- Sheldrick, G.M., Schneider, T.R., 1997. SHELXL: high-resolution refinement. *Method. Enzymol.* 277, 319–343.
- Sun, H.D., Huang, S.X., Han, Q.B., 2006. Diterpenoids from *Isodon* species and their biological activities. *Nat. Prod. Rep.* 23, 673–698.
- Sun, H.D., Lin, Z.W., Niu, F.D., Lin, L.Z., Chai, H., Pezzuto, J.M., Cordell, G.A., 1994. Cytotoxic diterpenoids from *Isodon megathyrus*. *J. Nat. Prod.* 57, 1424–1429.
- Sun, H.D., Xu, Y.L., Jiang, B., 2001. Diterpenoids from *Isodon* Species. Science Press, Beijing (p. v).
- Wang, X.R., Hu, H.P., Wang, H.P., Wang, S.Q., Shinichi, U., Tetsuro, F., 1994.

- Nervosanin A and B, and *ent*-kauranoids from *Isodon nervosus*. *Phytochemistry* 37, 1367–1370.
- Wang, W.G., Du, X., Li, X.N., Wu, H.Y., Liu, X., Shang, S.Z., Zhan, R., Liang, C.Q., Kong, L.M., Li, Y., Pu, J.X., Sun, H.D., 2012. New bicyclo[3.1.0]hexane unit *ent*-kaurane diterpenoid and its seco-derivative from *Isodon eriocalyx* var. *laxiflora*. *Org. Lett.* 14, 302–305.
- Wong, L.L., Liang, Z.T., Chen, H.B., Zhao, Z.Z., 2015. Ingredient authentication of commercial xihuangcao herbal tea by a microscopic technique combined with UPLC-ESI-QTOF-MS/MS. *Anal. Methods* 7, 4257–4268.
- Wu, H.Y., Zhan, R., Wang, W.G., Jiang, H.Y., Du, X., Li, X.N., Li, Y., Pu, J.X., Sun, H.D., 2014. Cytotoxic *ent*-kaurane diterpenoids from *Isodon wikstroemioides*. *J. Nat. Prod.* 77, 931–941.
- Xiang, W., Na, Z., Li, S.H., Li, M.L., Li, R.T., Tian, Q.E., Sun, H.D., 2003. Cytotoxic diterpenoids from *Isodon enanderianus*. *Planta Med.* 69, 1031–1035.
- Xu, Y.L., Kubo, I., Tang, C.S., Zhang, F.L., Sun, H.D., 1993. Diterpenoids from *Rabdosia forrestii*. *Phytochemistry* 34, 461–465.
- Yan, F.L., Xie, R.J., Yin, Y.Y., Zhang, Q., 2012. Serrin D, a new *ent*-kaurane diterpenoid from *Isodon serra*. *J. Chem. Res.* 36, 523–524.
- Yan, F.L., Zhang, L.B., Zhang, J.X., Sun, H.D., 2007. Two new diterpenoids and other constituents from *Isodon serra*. *J. Chem. Res.* 362–364.
- Yang, J., Wang, W.G., Wu, H.Y., Du, X., Li, X.N., Li, Y., Pu, J.X., Sun, H.D., 2016. Bioactive enmein-type *ent*-kaurane diterpenoids from *Isodon phyllostachys*. *J. Nat. Prod.* 79, 132–140.
- Zhao, A.H., Zhang, Y., Xu, Z.H., Liu, J.W., Jia, W., 2004. Immunosuppressive *ent*-kaurene diterpenoids from *Isodon serra*. *Helv. Chim. Acta* 87, 3160–3166.
- Zhong Yao Da Ci Dian, 1997. Jiang Shu New Medical College. Shanghai People Press, Shanghai, p. 2511.
- Zheng, Q., Cui, J.M., Fu, H.Z., 2011. Studies on chemical constituents of *Rabdosia serra*. *China J. Chin. Mater. Med.* 36, 2203–2206.